Plasma-Wall Transition in an Oblique Magnetic Field

R. Chodura

IPP 1/194 October 1981

MAX-PLANCK-INSTITUT FÜR PLASMAPHYSIK

8046 GARCHING BEI MÜNCHEN

MAX-PLANCK-INSTITUT FÜR PLASMAPHYSIK

GARCHING BEI MÜNCHEN

Plasma-Wall Transition in an Oblique Magnetic Field

R. Chodura

IPP 1/194 October 1981

Die nachstehende Arbeit wurde im Rahmen des Vertrages zwischen dem Max-Planck-Institut für Plasmaphysik und der Europäischen Atomgemeinschaft über die Zusammenarbeit auf dem Gebiete der Plasmaphysik durchgeführt.

IPP 1/194 R. Chodura

Plasma-Wall Transition in an Oblique Magnetic Field

English

Abstract

This paper studies the effect of a magnetic field on the transition layer between a plasma and an absorbing wall. A numerical model is used which simulates the motion of plasma particles in the electric and magnetic fields for a prescribed particle influx at the plasma boundary. Bohm's condition for the existence of a monotonic profile of the layer is generalized.

The transition layer proves to have a double structure comprising a quasineutral magnetic presheath preceding the electrostatic Debye sheath. The magnetic presheath scales with the ion gyro radius at the sound speed and with the angle of the magnetic field. The total electric potential drop between plasma and wall proves to be fairly insensitive to the magnitude and angle of the magnetic field.

1. Introduction

The steady state of a plasma device is to a large extent determined by the boundary condition at the material wall, i.e. limiter, divertor etc. Since processes at the plasma-wall boundary are rather complex, it is desirable to simulate these processes in a numerical model in order to get an insight into the relative importance and the interaction of different effects.

One of the characteristic features of the transition between plasma and an absorbing wall is the build-up of an electric space charge potential at the plasma edge. This potential in an otherwise field-free boundary layer has been investigated theoretically for a long time (see /1/ for further literature). But in many practical cases, e.g. in tokamaks, the boundary layer is interspersed with a magnetic field hitting the wall (limiter, divertor plate) at some angle between normal and nearly grazing. The limiting case of a field parallel to the wall was treated recently /2/. The present paper intends to describe a kinetic model for a plasma boundary region in a magnetic field of arbitrary strength and direction and to study the dependence of the edge potential and particle flow on the magnetic field.

The reason for the space charge potential is the different acceleration of electrons and ions at the plasma edge by their respective thermal pressures. Electrons, in general, are too fast and must be slowed down by the electric field, ions are accelerated, so that the electric field effects equal fluxes of negative and positive charges to the wall.

On their way out, plasma particles transverse three distinct regions: in the inner region the electric field is relatively weak, and plasma particles are accelerated along the magnetic field. The plasma is quasineutral. In the second region, the electric field which is perpendicular to the wall, is strong enough to deflect the plasma particles from their direction parallel to the field (if this direction is different from perpendicular). Particles experience the action of the magnetic field. The size of this region depends on the ion gyro radius and angle of the magnetic field to the wall normal. The plasma is still quasineutral. This region is referred to as "magnetic presheath". The third region is the electrostatic sheath region. The electric field exceeds the action of the magnetic

field; the plasma is non-neutral. Its scale length is the Debye length.

In the next section we describe a simple numerical particle model to calculate the particle flow and the electric field in the plasma-wall region together with a fluid approximation for the magnetic presheath. In section 4 we discuss the plasma behaviour in the magnetic presheath and sheath region in more detail.

2. Model

a) Kinetic Model

Figure 1 shows the geometry of the model for the plasma-wall transition. The plasma state is assumed to depend on the coordinate x perpendicular to the wall only. The electric field $E = -\partial\phi/\partial x$ is parallel to the x direction and the static, homogeneous magnetic field B includes an angle ψ to x. At x = L there is a particle absorbing wall. The plane x = 0 (which is not very well defined) separates the bulk plasma $x < 0$ with weak electric field from the transition zone $x > 0$ to the wall, where E is appreciable. The bulk plasma is assumed to contain sources which maintain stationary particle fluxes across x = 0. The transition zone $x > 0$ is assumed to be collisionless.

The motion of ions and electrons in their self-consistent electric and prescribed magnetic fields are calculated by a particle-in-cell method. Thus, in the calculation area $0 \leq x \leq L$ the temporal development of the system is described by ($\dot{} = d/dt$, $' = \partial/\partial x$)

$$\begin{aligned} m_{ie}\,\dot{\underline{v}}_{ie} &= \pm q_{ie}\left(\underline{E} + \underline{v}_{ie} \times \underline{B}\right) \\ \dot{x}_{ie} &= v_{x,\,ie} \\ E' &= q_i n_i - q_e n_e \end{aligned} \qquad (1)$$

where particle densities n_i and n_e are calculated from the momentary position of the particles.

The velocity distribution of particles streaming into the calculation area are prescribed as boundary conditions: at x = 0 a time-independent Maxwellian distribution shifted for the ions by a velocity $\underline{v}_{i0}$ along $\underline{B}$ is adopted;

$$f^{0}_{ie} = f_{ie}\left(x=0,\, v_x > 0\right) = n^{0}_{ie}\left(m_{ie}/2\pi T^{0}_{ie}\right)^{3/2} \exp\left\{-m_{ie}/(2T^{0}_{ie})\left(\underline{v}-\underline{v}_{i0}\right)^2\right\} \qquad (2)$$

with $\underline{v}_{io}$ parallel to $\underline{B}$.
At x = L a total absorbing wall is assumed;

$$f_{ie}\,(x=L,\ v_x<0) = 0 \quad , \tag{3}$$

Of course, other conditions as partial reflection, secondary emission etc. could be applied as well.

The electric field at x = 0 at a time t is determined by the charge imbalance $Q_i^P - Q_e^P$ in the bulk plasma x < 0 at this time. Assuming neutrality in the bulk plasma at the starting point t = 0, this imbalance is connected with the difference in time-integrated flux F through the plane x = 0, so that

$$E\,(x=0,t) = Q_i^P - Q_e^P = -\int_0^t d\tau\,\left(F_{xi}(0,\tau) - F_{xe}(0,\tau)\right)$$

where

$$F_{x,ie} = \int_{-\infty}^{\infty} d^3v\ v_x\ f_{ie} \tag{4}$$

The initial condition of the system is an empty computation area. Owing to the time independence of the boundary conditions for the particles (2) and (3), the system becomes stationary after some time. Condition (4) enforces equal fluxes of ions and electrons, which, in steady state also become space-independent.
Still, not every steady state of the system is an acceptable solution of the plasma-wall transition problem. It is further required that E (x = 0) and its derivatives be nearly zero, so that also $n_i \approx n_e$ and $n_i' \approx n_e' \approx 0$ at x = 0. This can only be satisfied for boundary conditions (2) with certain values of $\underline{v}_o$, T_{eo} and T_{io}.
It is well known from the theory of plasma-wall transition without magnetic field that in order to get monotonic profiles which smoothly join the bulk plasma region, one has to satisfy the so-called Bohm condition /3/, e.g.

$$v_{io}^2 \geq T_{eo} / m_i \tag{5}$$

for cold ions, $T_{io} = 0$. The generalization of the Bohm condition to the case with magnetic field is given in the next section. The model is tested by comparing the wall potential as determined in the model with the theoretical value for perpendicular magnetic field as a function of the ratio of instreaming fluxes F_{io} / F_{eo}

where $F_{ie}^{o} = \int_{v_x > 0} d^3v \; v_x \; f_{ie}^{o}$. (Fig. 2).

L was changed from 5 and 20 Debye lengths in order to check the independence of the result on the system length.

In the following the model was used to find general properties and scaling laws of the transition layer. So an artificial mass ratio $m_i/m_e = 100$ was used to save computer time.

b. Fluid Approximation

Under certain conditions (for instance small deviation from thermal equilibrium for electrons, not too hot ions) the kinetic model can be replaced by the simpler tow-fluid model for ions and electrons. This model gives at least qualitatively correct results and is especially appropriate for the magnetic presheath.
Let $\underline{V}$ be the fluid velocity of one species

$$\underline{V} = \frac{1}{n} \int d^3v \; \underline{v} \; f \; .$$

The continuity and momentum equations for ions and electrons are

$$\left(n_{ie} \; V_{x,ie}\right)' = 0 \qquad (6)$$

$$m_{ie} \; \underline{V}_{ie} \cdot \nabla \underline{V}_{ie} = \pm \, q_{ie} \left(\underline{E} + \underline{V}_{ie} \times \underline{B}\right) - \nabla p_{ie} / n_{ie} \; . \qquad (7)$$

As closure condition for the fluid description

$$\nabla p_{ie} = \gamma_{ie} \; T_{ie} \; \nabla n_{ie} \qquad (8)$$

is assumed.
E is given by Poisson's equation

$$E' = q_i n_i - q_e n_e \qquad (9)$$

For electron fluid velocity V_e small compared with the thermal velocity $c_e = (T_e/m_e)^{1/2}$ the x-momentum equation simply becomes

$$- q_e E - \gamma_e T_e n_e' / n_e = 0 \qquad (10)$$

Furthermore, if the gradient length is large compared with the Debye length, the system is quasinuetral, i.e.

$$n_i \approx n_e , \quad V_{xi} \approx V_{xe} \qquad (11)$$

and the electric field is determined by eq. (10) instead of eq. (9).

3. Results

Figure 3a, b shows x-profiles of the potential ϕ for different angles of incidence ψ of the magnetic field and for cold and warm ions as obtained from the kinetic model. For $\psi > 0$ the profile is composed of two parts: a slowly falling part which is called "magnetic presheath" in the following, succeeded by the sharp fall of the proper sheath region at the wall, which is 5 to 10 Debye lengths λ_D wide. For increasing angle the potential drop in the presheath becomes larger. For cold ions and medium angles an oscillation in the presheath is superimposed, which will be discussed in the next section. The total potential drop ϕ_w from the plasma edge to the wall for different angles ψ and strengths of the magnetic field is shown in Fig. 4a, b. This dependence is rather weak.

For a discussion of the structure of the plasma-wall transition layer it is more appropriate to inspect the profile of the flow velocities V_x. These profiles are shown in Fig. 5a, b for an angle $\psi = 60^\circ$ and two ion temperatures.

Ignoring for the moment the oscillations in the case $T_i = 0$, it is obvious that the transition layer has a double structure of a broad quasineutral ($V_{xi} \approx V_{xe}$) presheath and a relatively narrow Debye sheath with charge separation ($V_{xe} > V_{xi}$). The thickness of the presheath depends on the magnetic field, while the Debye sheath is independent of B.

For a smooth start of the profile at the left (plasma) side the flow velocity of the instreaming plasma V_{xo} has to exceed a certain limit, i.e.

$$V_{xo} > c_s \cos\psi \;, \text{ i.e. } |V_o| > c_s \;, \quad c_s^2 = (\gamma_i T_i + \gamma_e T_e)/m_i \tag{12}$$

otherwise the system would develop an electric field at the left edge to accelerate the incoming ions to this limit. This is the expression of Bohm's condition in the numerical model.
In the following, this condition together with other details of the transition layer are discussed.

4. Discussion

a. Bohm's Condition and Oscillations in the Magnetic Presheath

Let us envisage a time-independent disturbance ~~$\propto$~~ $\exp(ikx)$ with wave number k in the x direction of an equilibrium state

$$\underline{V}_i = \underline{V}_o \;, \quad \underline{V}_o \parallel \underline{B} \;, \quad n_i = n_e = n_o \;, \quad E = 0 \;.$$

Equations (6) to (8) for ions together with equations (9) and (10) yield a dispersion relation

$$k^2 \lambda_D^2 = - \frac{(k^2 V_{xo}^2 - \Omega_x^2)(V_{xo}^2 - c_s^2) - \Omega_z^2 V_{xo}^2}{(k^2 V_{xo}^2 - \Omega_x^2)(V_{xo}^2 - c_i^2) - \Omega_z^2 V_{xo}^2} \;, \tag{13}$$

$$\underline{\Omega} = e\underline{B}/m_i \;, \quad c_i^2 = \gamma_i T_i / m_i \;, \quad c_s^2 = (\gamma_i T_i + \gamma_e T_e)/m_i$$

This dispersion relation as a function of V_{x_0} is plotted in Fig. 6a,b for $\Psi = 60^o$, $T_{io} = T_{eo}$ and $T_i = 0$. There are two modes 1 and 2 and two asymptotic branches, i.e. an electrostatic ion cyclotron mode I

$$k_I^2 = \Omega_x^2 / V_{x_0}^2 + \Omega_z^2 \left(V_{x_0}^2 - c_s^2 \right) \qquad (14)$$

and an ion acoustic branche II

$$k_{II}^2 \lambda_D^2 = - \left(V_{x_0}^2 - c_s^2 \right) \Big/ \left(V_{x_0}^2 - c_i^2 \right) . \qquad (15)$$

Mode 1 starts for small k as an ion cyclotron mode and changes at $V_{x_0} = c_s$ to the ion acoustic branch, while mode 2 does the opposite. The ion cyclotron branch I is quasineutral. Thus, mode 1 is quasineutral for $V_{x_0} < c_s$, and mode 2 for $V_{x_0} > c_s$.

For $\Psi = 0$, the ion acoustic and cyclotron modes are decoupled. As one can see from the diagram, a monotonic disturbance, i.e. $k^2 < 0$ is only possible for condition (12). This is Bohm's condition in the case of an oblique magnetic field. It is the same as in the magnetic field-free case provided V_o is taken along the magnetic field.

The scale length of variation in the magnetic presheath is of the order c_s/Ω with some dependence on Ψ . In the sheath, this scale length is the Debye length λ_D .

The pronounced oscillations in Figs. 3b and 5b for $\Psi = 60^o$ are due to the excitation of an ion acoustic mode 2 with

$$0 \leq k_2^2 \lambda_D^2 \leq 3 \qquad \text{for} \qquad c_s \cos\Psi < V_{x_0} < c_s \, . \qquad \text{(Fig. 6b).}$$

For the same angle but $T_{io} = T_{eo}$ (Fig. 6a), there is no oscillating mode $k^2 > 0$ for $c_s \cos\Psi < V_{x_0} < c_s$, hence the corresponding profiles in Figs. 3a and 5a are monotonic.

b. Scaling of the Magnetic Presheath

As is shown in Fig. 5, the magnetic presheath is quasineutral. It can, therefore, be described by equations (6) to (8) for the ions together with equations (10) and (11) for the electrons. By elimination and integration one gets the ordinary differential equation for V_x :

$$(V_x^2 - c_s^2)V_x'' + (V_x^2 + c_s^2)V_x'^2/V_x + \Omega^2 V_x + \Omega_x^2 c_s^2/V_x = \text{const} \tag{16}$$

Introducing

$$s = (x - L)\,\Omega/c_s \;,\quad y = V_x/c_s \;,\quad y_0 = V_{x0}/c_s \;,$$

$$u = (dy/ds)^2 \;,\quad u_0 = u(y = y_0) \;,\quad C = -\text{const}/(\Omega^2 c_s)$$

one finds the integral of equation (16):

$$u(y) = \frac{y^2}{(1-y^2)^2}\left\{\frac{(1-y_0^2)^2}{y_0^2}u_0 + \left[\cos^2\psi\,\frac{y+y_0}{y_0^2 y^2} + \frac{2C}{y_0 y} - 2C - (y+y_0)\right](y-y_0) + 2\sin^2\psi\,\ln(y/y_0)\right\} \tag{17}$$

As boundary condition at the plasma side we assume an instreaming flow velocity at the Bohm limit

$$y = y_0 = \cos\psi$$

and

$$y' = y'' = 0$$

from which $$u_0 = 0 \;,\quad C = -2y_0 \;. \tag{18}$$

As right-hand boundary condition we choose

$$x = L \;,\quad y = 1 \tag{19}$$

This choice is arbitrary and is justified afterwards from the results.

Integrating equation (17) for these boundary conditions

$$s = -\int_{y}^{1} dw \Big/ \sqrt{u(w)} \tag{20}$$

yields the profiles $y(s,\psi)$ of Fig. 7. In Fig.5a,b the profile for $\psi = 60^{\circ}$ (labelled with V_x) is compared with the results from the kinetic model. As can be seen, the solution of the fluid equations (17) to (20) represents the course of V_x in the magnetic presheath fairly well. The coincidence ceases in the Debye sheath.

At the first rise of y in the magnetic presheath, i.e. for $y - y_0 \ll 1$, equation (17) with (18) is approximated by

$$u \approx \alpha (y-y_0)^3 \quad , \quad \alpha = 2/[3y_0(1-y_0^2)] \tag{21}$$

Interpreting equation (21) in undefined form

$$s = \int dw \Big/ \sqrt{u(w)} + \text{const} \tag{22}$$

yields the asymptotic profile of y for $x \to -\infty$ in the magnetic presheath

$$y/y_0 - 1 = d_u^2/(x - \text{const})^2 \tag{23}$$

with the scale length

$$d_u = \sqrt{6}\, c_s/\Omega \sin\psi \, . \tag{24}$$

Thus, the scale length d_u increases with increasing angle ψ as the component B_z of the magnetic field.

c. Potential Differences in the Transition Layer

As Fig. 4 shows, the total potential drop over the transition layer ϕ_w , i.e. the total energy gain or loss of ions and electrons across the layer, is nearly independent of the magnitude and direction of the magnetic field, being determined only by the ratio of instreaming particle fluxes F_o , i.e.

$$e\phi_w / T_e \sim \ln (F_{io} / F_{eo}) .$$

The potential drop over the magnetic presheath ϕ_s , on the other hand, is dependent on Ψ : from equations (6) and (10) it follows that

$$e\phi_s / T_e \approx - \ln (V_{xs} / V_{xo})$$

where $V_{xs} = V_x(x_s)$ and x_s is the position of the edge of the presheath $\approx L$ – some Debye lengths. From Fig. 7 this ratio is seen to increase monotonically with Ψ and c_s / Ω . Accordingly, the potential drop across the Debye sheath decreases with growing Ψ and c_s / Ω .

The case $\Psi = 90^o$ is singular since both ion and electron fluxes to the wall vanish, $F_{xi} = F_{xe} = 0$. Due to their larger gyro radii ions can penetrate the field farther. Thus the potential becomes positive.

5. Conclusion

The transition layer between a plasma and an absorbing wall is shown to be composed of a magnetic presheath which scales with the magnetic field as c_s / Ω and the electrostatic Debye sheath of several Debye lengths. The total potential drop between plasma and wall is fairly insensitive to the magnetic field.

Literature

/1/ G.A. Emmert, R. M. Wieland, A.T. Mense, J.N. Davidson, Phys. Fluids 23, 803 (1980)

/2/ U. Daybelge, B. Bein, Phys. Fluids 24, 1190 (1981)

/3/ D. Bohm in "The Characteristics of Electrical Discharges in Magnetic Field", Eds. A. Guthrie, R.K. Wakerling (McGraw-Hill Book Company, Inc., New York, 1949, Chap. 3, p. 77)

Acknowledgement

The author wishes to thank Drs. K. Lackner and U. Daybelge for helpful discussions.

Figure Captions

Fig. 1: Geometry of the model

Fig. 2: Model test case: wall potential ϕ_w for perpendicular magnetic field as function of the ratio of ion and electron in fluxes F_{io}/F_{eo} and for two different system lengths L as compared to the theoretical value $\ln\left(F_{io}/F_{eo}\right)$.

Fig. 3: Potential distribution $\phi(x)$ for different angles ψ of the magnetic field. (a) $T_{io} = T_{eo}$; (b) $T_{io} = 0$

Fig. 4: Wall potential ϕ_w at $\psi = 60^o$ for
(a) varying angles ψ
(b) varying magnetic field strengths, expressed by the ratio of electron gyro frequency ω to plasma frequency ω_p.

Fig. 5: Flow velocity of ions and electrons $V_{x,ie}(x)$ for $\psi = 60^o$ from the model. The dashed curve represents the quasineutral fluid approximation (6) to (8) and (10) for the magnetic presheath with $\gamma_i = 2$, $\gamma_e = 1$. (isothermal electrons)
(a) $T_{io} = T_{eo}$, (b) $T_{io} = 0$

Fig. 6: Dispersion relation k^2 (V_{xo}) for the two modes 1 and 2 from linearized fluid equations (6) to (10).
The asymptotic modes are:
I ... electrostatic ion cyclotron mode,
II... ion acoustic mode.
(a) $T_{io} = T_{eo}$; (b) $T_{io} = 0$

Fig. 7: Quasineutral flow approximation for the magnetic presheath. The approximation holds except for the sheath region extending some Debye lengths ahead of x = L

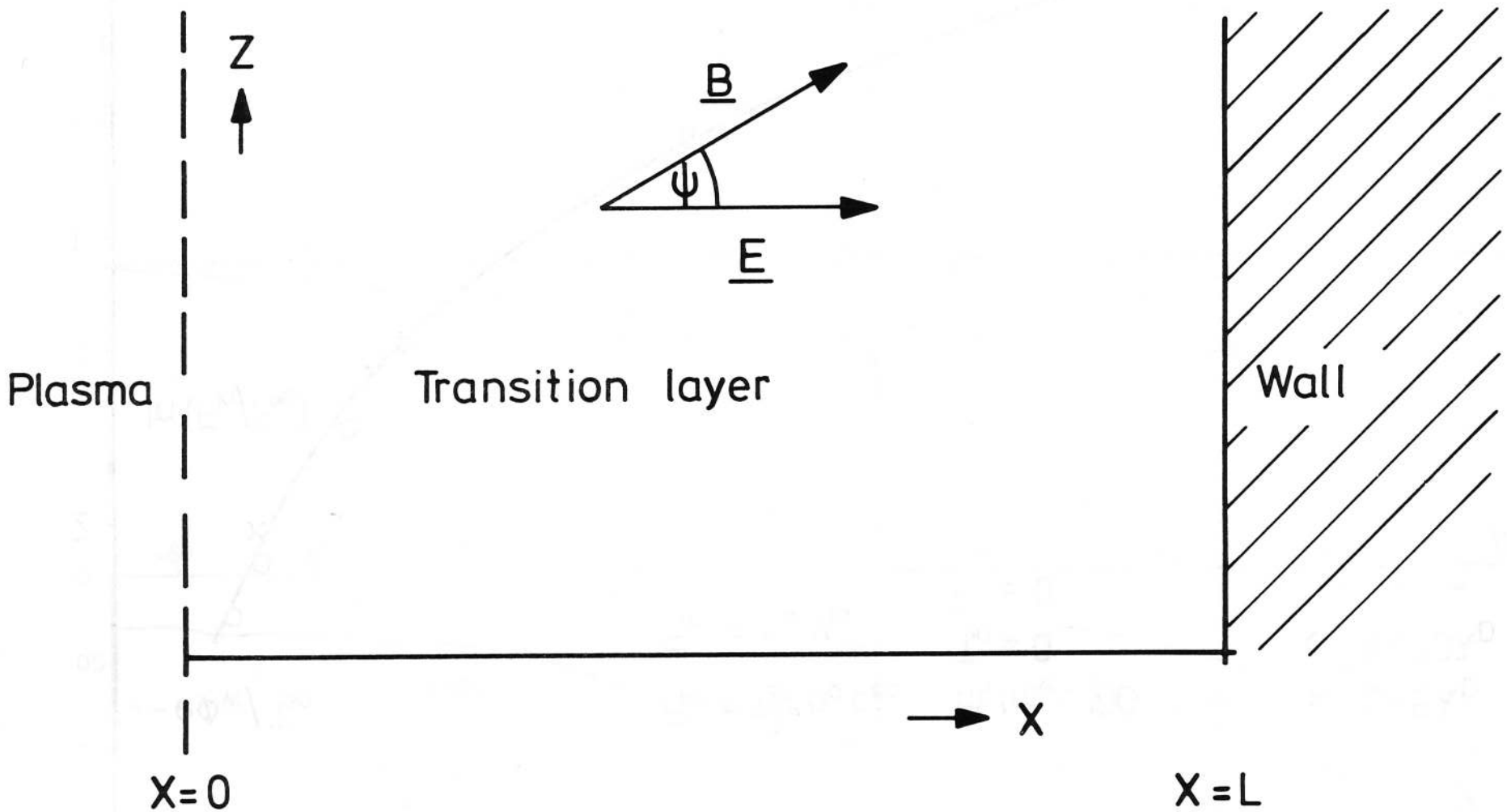
Z
B
ψ
E
Plasma
Transition layer
Wall
X
X=0
X=L

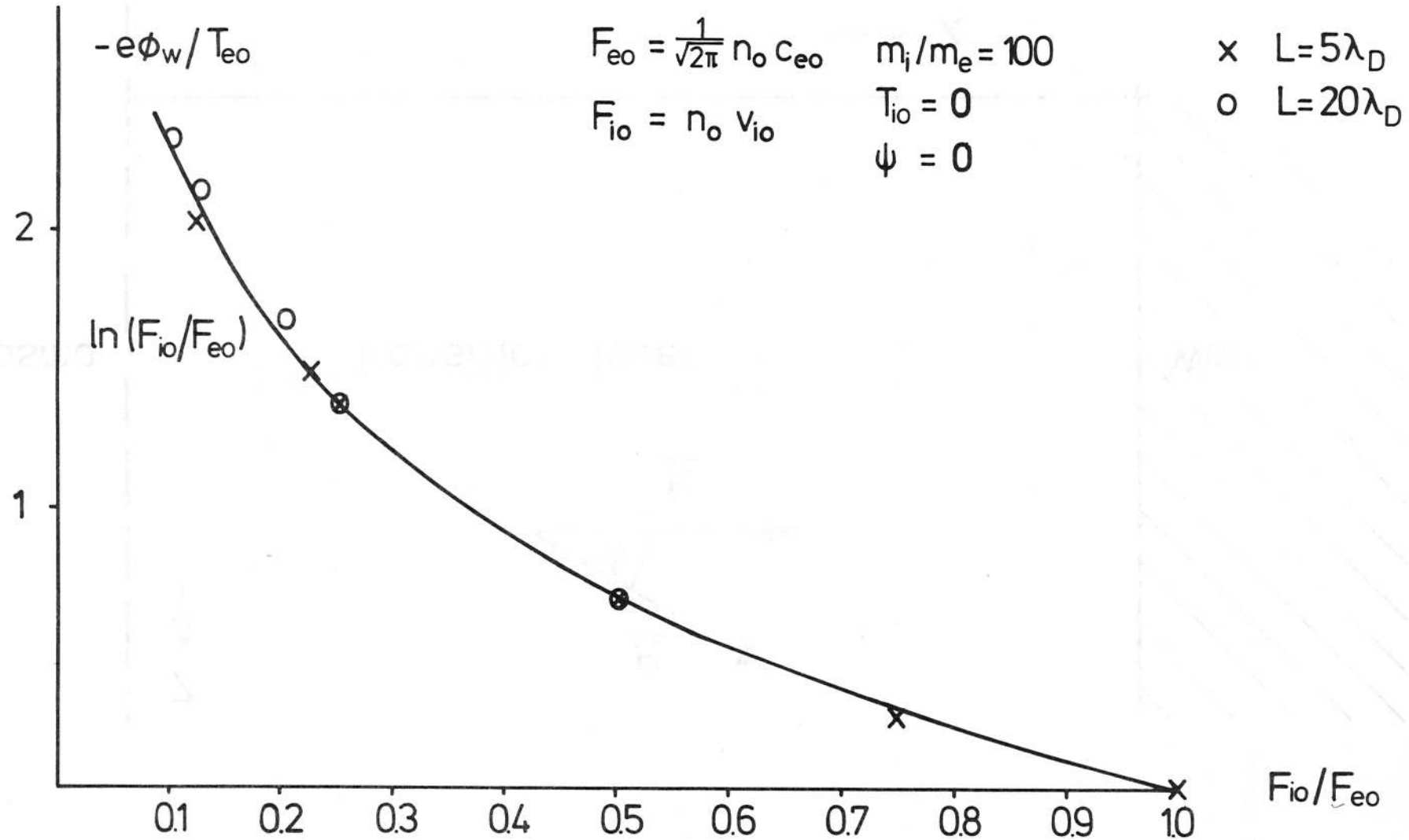
$-e\phi_w / T_{eo}$
$F_{eo} = \frac{1}{\sqrt{2\pi}} n_o c_{eo}$
$F_{io} = n_o v_{io}$
$m_i/m_e = 100$
$T_{io} = 0$
$\psi = 0$
x $L = 5\lambda_D$
o $L = 20\lambda_D$
$\ln (F_{io}/F_{eo})$
2
1
0.1
0.2
0.3
0.4
0.5
0.6
0.7
0.8
0.9
1.0
F_{io}/F_{eo}

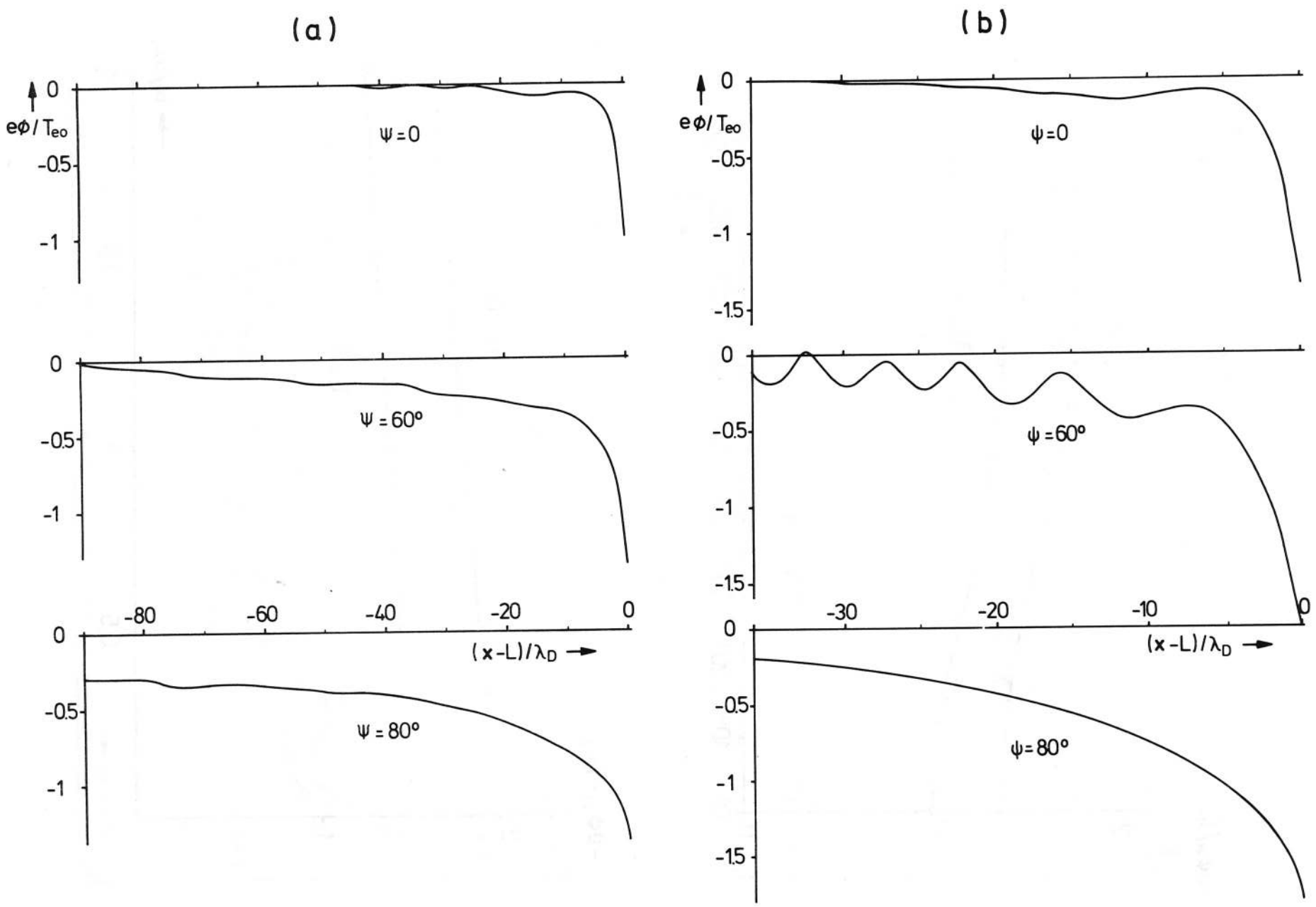
(a)
(b)
eφ/ Teo
0
-0.5
-1
-1.5
ψ = 0
ψ = 60°
ψ = 80°
-80
-60
-40
-20
-30
-10
(x-L)/λD

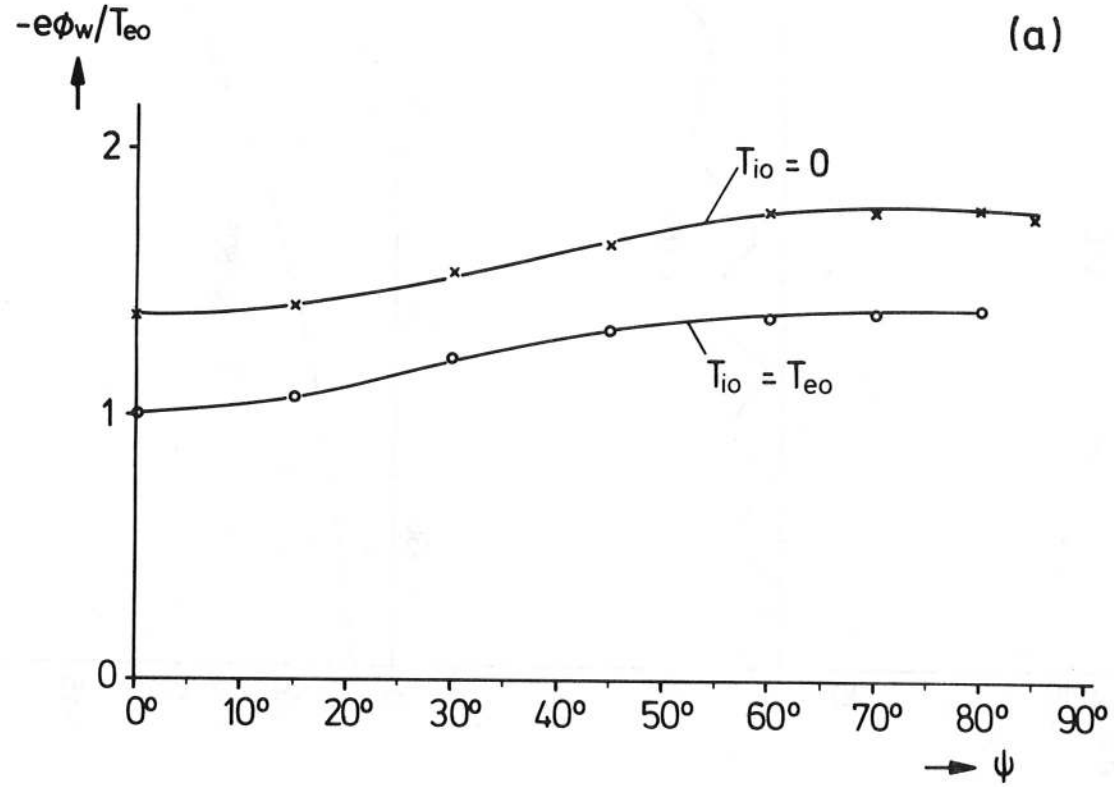
-eφw/Teo
(a)
2
1
0
Tio = 0
Tio = Teo
0°
10°
20°
30°
40°
50°
60°
70°
80°
90°
ψ

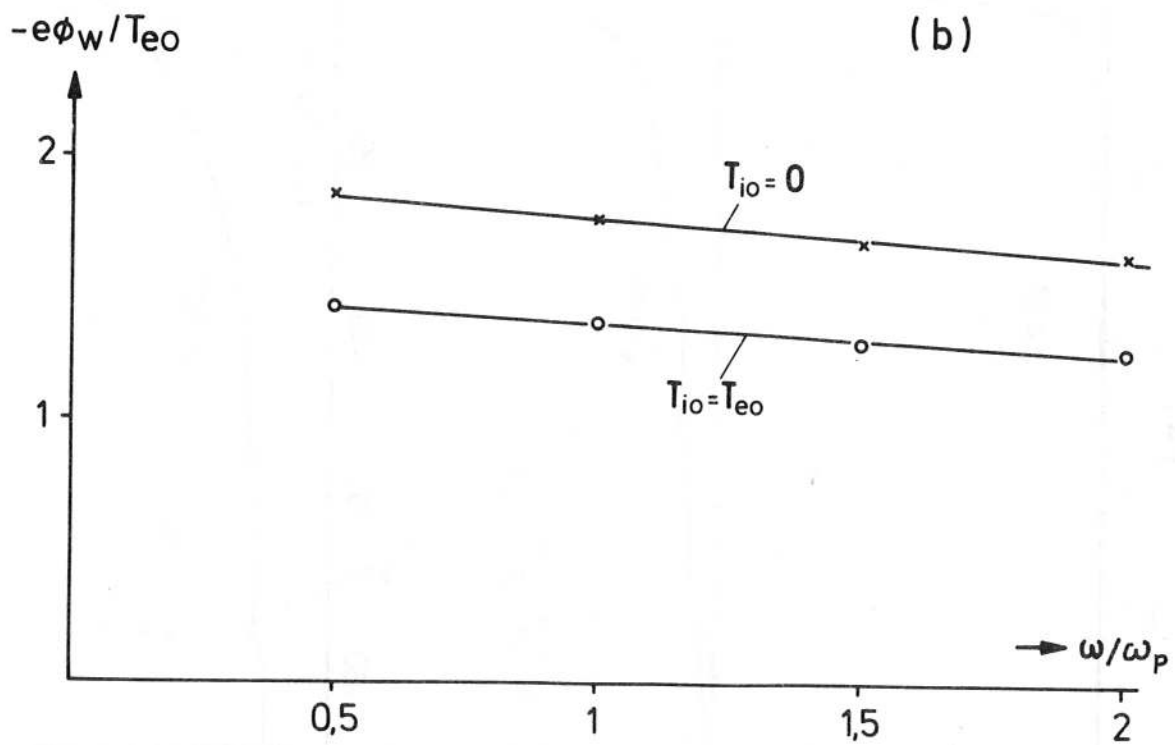
-eφw/Teo
(b)
2
1
Tio = 0
Tio = Teo
0,5
1
1,5
2
ω/ωp

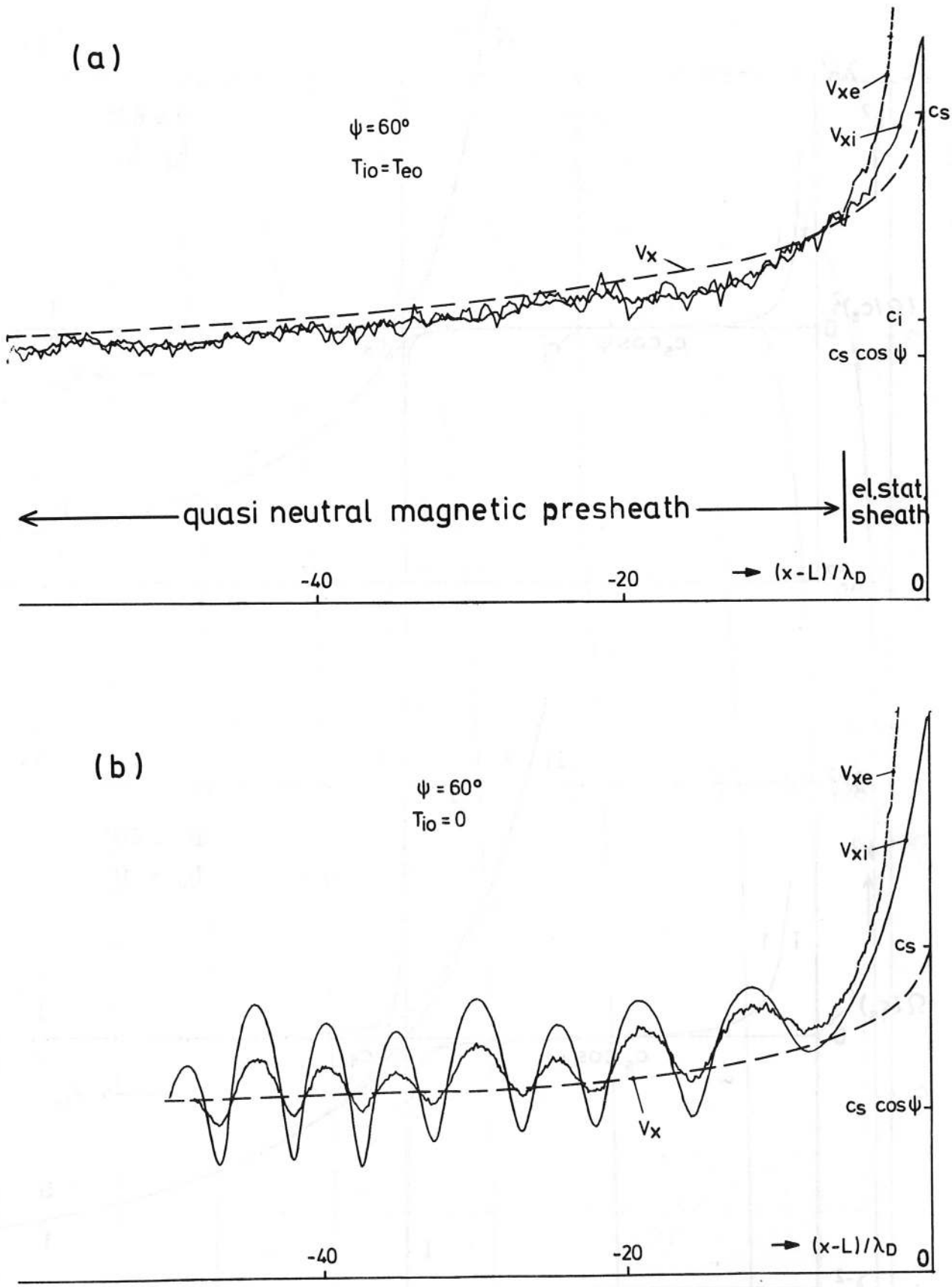
(a)
ψ = 60°
Tio = Teo
Vxe
Vxi
Vx
cs
ci
cs cos ψ
quasi neutral magnetic presheath
el.stat. sheath
-40
-20
(x-L)/λD
0
(b)
ψ = 60°
Tio = 0
Vxe
Vxi
Vx
cs
cs cosψ
-40
-20
(x-L)/λD
0

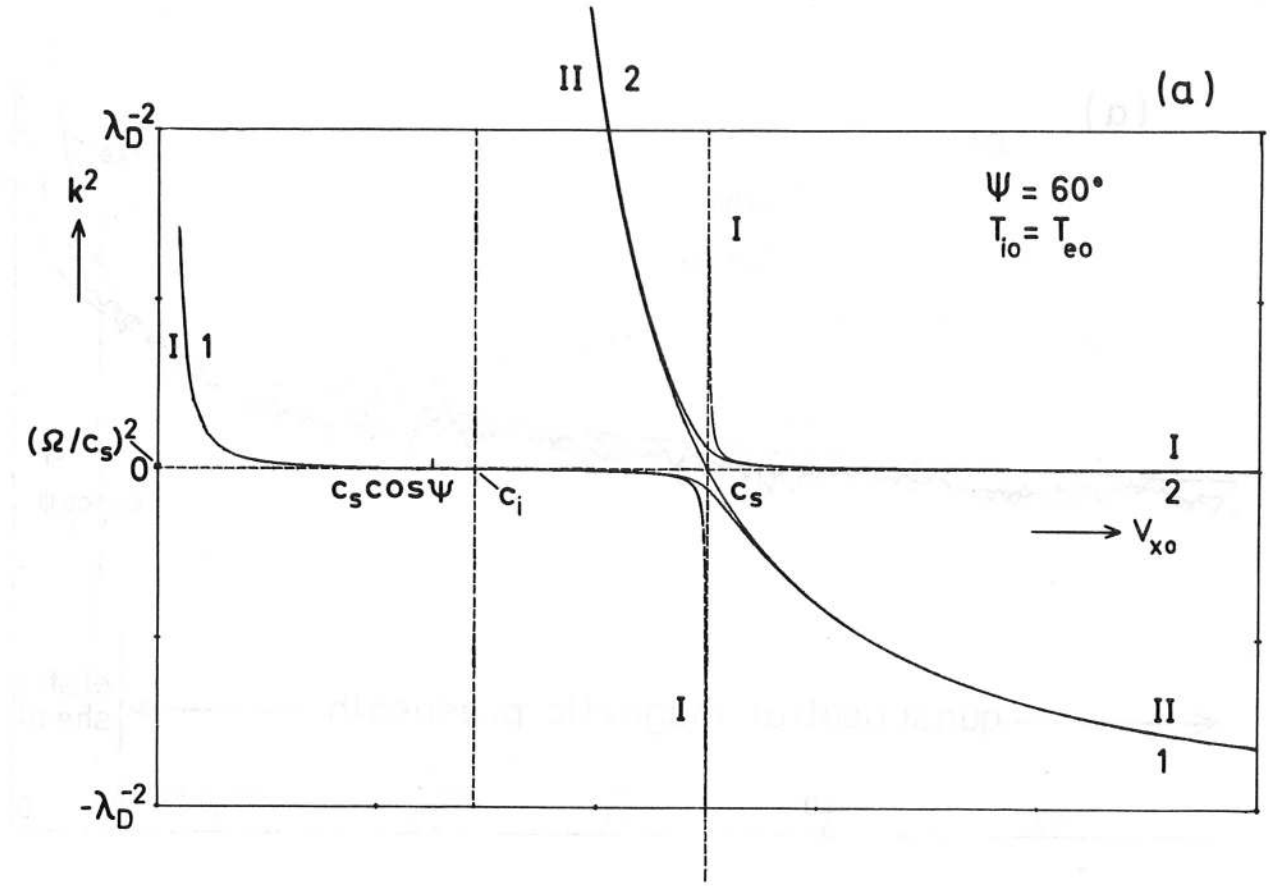
(a)
II 2
λ_D^{-2}
k^2
$\Psi = 60°$
$T_{io} = T_{eo}$
I
I 1
$(\Omega/c_s)^2$
0
I
2
$c_s \cos\Psi$
c_i
c_s
V_{xo}
I
II
1
$-\lambda_D^{-2}$

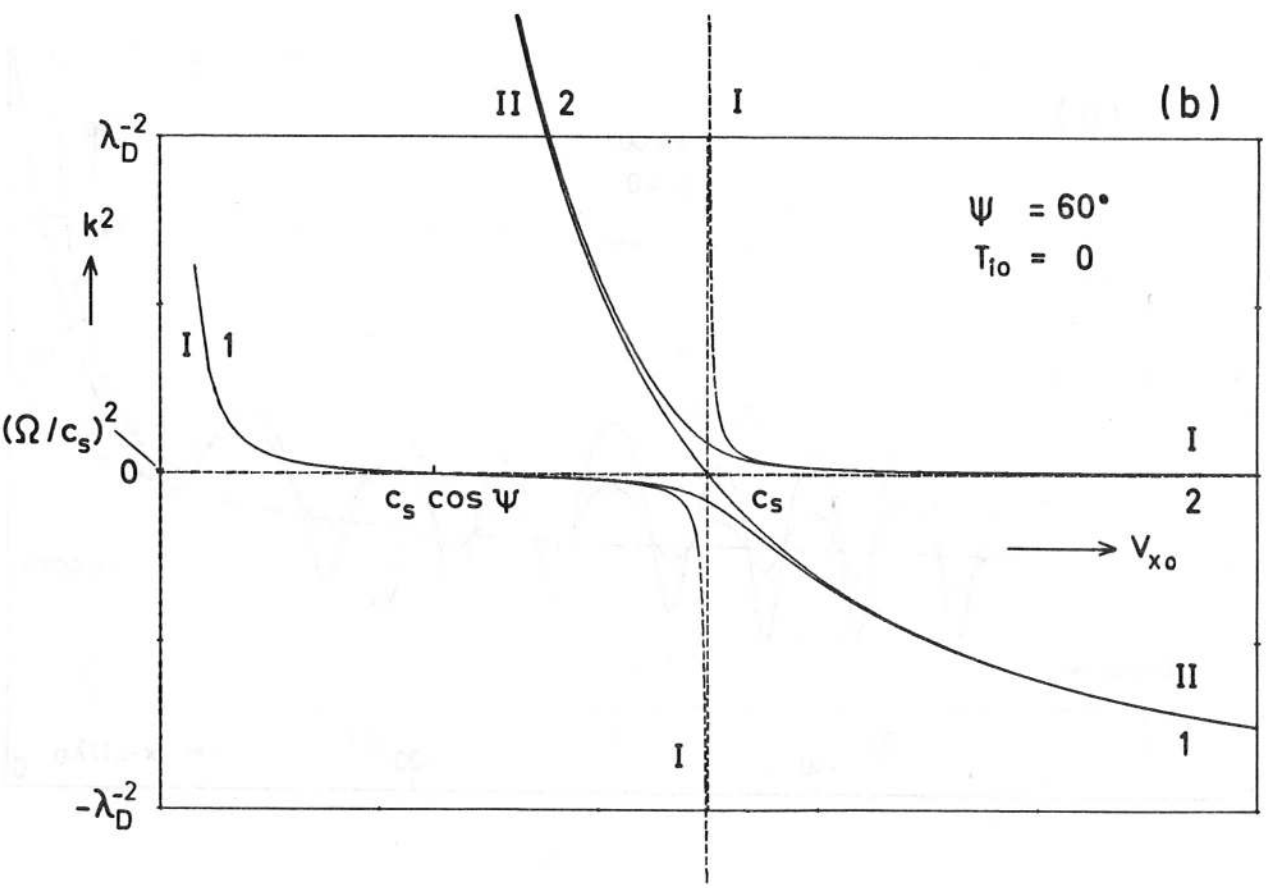
(b)
II 2
I
λ_D^{-2}
k^2
$\Psi = 60°$
$T_{io} = 0$
I 1
$(\Omega/c_s)^2$
0
I
2
$c_s \cos\Psi$
c_s
V_{xo}
II
1
I
$-\lambda_D^{-2}$

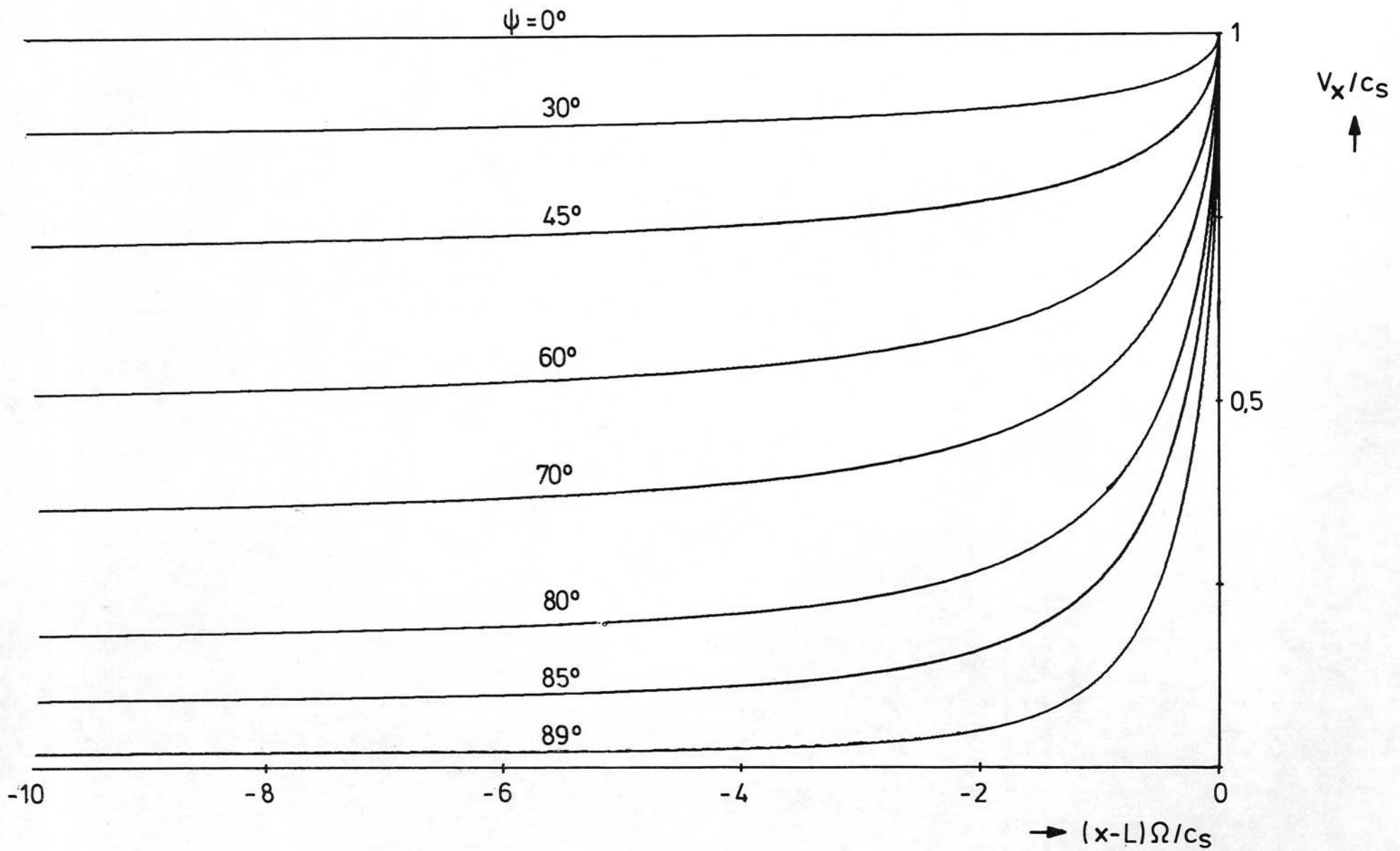
ψ = 0°
30°
45°
60°
70°
80°
85°
89°
1
0,5
V_x/c_s
-10
-8
-6
-4
-2
0
$(x-L)\Omega/c_s$